TLR13 Recognizes Bacterial 23S rRNA Devoid of Erythromycin Resistance–Forming Modification

Marina Oldenburg *et al.*

Science **337**, 1111 (2012);
DOI: 10.1126/science.1220363

Science (print ISSN 0036-8075; online ISSN 1095-9203) is published weekly, except the last week in December, by the American Association for the Advancement of Science, 1200 New York Avenue NW, Washington, DC 20005.

Table 2. Minimum inhibitory concentrations of various antibiotics toward both multidrug resistant soil isolates and *E. coli* clones expressing selected resistance genes (all concentrations are μg/mL). AX, amoxicillin; CA, carbenicillin; PE, penicillin; PI, piperacillin; CF, cefdinir; CH, chloramphenicol; SI, sisomicin; GE, gentamicin; MN, minocycline; OX, oxytetracycline; TE, tetracycline; and blank cells indicate inhibitory concentrations were not determined.

	AX	CA	PE	PI	CF	CH	SI	GE	MN	OX	TE
Ochrobactrum soil isolate	>2048	>2048	>2048	>2048	<16	512	512	512	<4	256	64
Pseudomonas soil isolate	>2048	>2048	>2048	>2048	>1024	1024	>1024	>1024	8	128	32
AB95_PI_68.1	>2048	>2048	2048	2048							
AB95_CH_33.1						256					
AB95_GE_3.3							>1024	>1024			
E. coli + empty vector control	<16	<32	64	16	<8	<8	<8	<8	<8	8	4

to soil organisms, of which many can cause nosocomial infection and may emerge as pathogens, akin to the rise of *A. baumannii*.

Powered by PARFuMS, a method for characterizing functional selections at <1% of the cost of traditional approaches (*19*), we describe antibiotic resistance genes found in nonpathogenic soil-dwelling bacteria and of all major mechanistic classes (*29*) with perfect nucleotide identity to many diverse human pathogens. We also show that multiple resistance genes are colocalized within long stretches of perfect nucleotide identity and are flanked by mobile DNA elements. These findings not only provide evidence for recent HGT of multidrug resistance cassettes between soil and clinic, but also a mechanism through which this exchange may have occurred.

The *Ochrobactrum* and *Pseudomonas* isolates originated from farmland soils fertilized with manure from antibiotic-treated livestock. However, our current study design did not enable a statistically significant association of pathogen-identical resistance genes to specific soils. Rather, our results highlight the fact that soil and pathogenic resistomes are not distinct, emphasizing the clinical importance of environmental resistance. Our new method provides the increased throughput required to power future studies to identify soil (*11*), aquatic (*5*), and other (*20*) environments prone to resistance exchange with human pathogens and to understand how specific anthropogenic practices influence the likelihood of this dissemination (*3*, *23*).

References and Notes

1. C. A. Arias, B. E. Murray, *N. Engl. J. Med.* **360**, 439 (2009).
2. R. Benveniste, J. Davies, *Proc. Natl. Acad. Sci. U.S.A.* **70**, 2276 (1973).
3. J. L. Martínez, *Science* **321**, 365 (2008).
4. L. Poirel, P. Kämpfer, P. Nordmann, *Antimicrob. Agents Chemother.* **46**, 4038 (2002).
5. L. Poirel, J. M. Rodriguez-Martinez, H. Mammeri, A. Liard, P. Nordmann, *Antimicrob. Agents Chemother.* **49**, 3523 (2005).
6. J. J. Farmer 3rd *et al.*, *J. Clin. Microbiol.* **13**, 919 (1981).
7. T. Stalder, O. Barraud, M. Casellas, C. Dagot, M. C. Ploy, *Front. Microbiol.* **3**, 119 (2012).
8. B. M. Marshall, S. B. Levy, *Clin. Microbiol. Rev.* **24**, 718 (2011).
9. V. M. D'Costa *et al.*, *Nature* **477**, 457 (2011).
10. V. M. D'Costa, K. M. McGrann, D. W. Hughes, G. D. Wright, *Science* **311**, 374 (2006).
11. H. K. Allen, L. A. Moe, J. Rodbumrer, A. Gaarder, J. Handelsman, *ISME J.* **3**, 243 (2009).
12. J. J. Donato *et al.*, *Appl. Environ. Microbiol.* **76**, 4396 (2010).
13. R. I. Aminov, R. I. Mackie, *FEMS Microbiol. Lett.* **271**, 147 (2007).
14. H. Heuer, H. Schmitt, K. Smalla, *Curr. Opin. Microbiol.* **14**, 236 (2011).
15. P. S. McManus, V. O. Stockwell, G. W. Sundin, A. L. Jones, *Annu. Rev. Phytopathol.* **40**, 443 (2002).
16. T. Kieser, M. J. Bibb, M. J. Buttner, K. F. Chater, D. A. Hopwood, *Practical Streptomyces Genetics* (John Innes Foundation, Norwich, UK, ed. 1, 2000).
17. J. Davies, D. Davies, *Microbiol. Mol. Biol. Rev.* **74**, 417 (2010).
18. H. W. Boucher *et al.*, *Clin. Infect. Dis.* **48**, 1 (2009).
19. Materials and methods are available as supplementary materials on *Science* online
20. M. O. Sommer, G. Dantas, G. M. Church, *Science* **325**, 1128 (2009).
21. G. Dantas, M. O. Sommer, R. D. Oluwasegun, G. M. Church, *Science* **320**, 100 (2008).
22. V. L. Clark, F. E. Young, *Antimicrob. Agents Chemother.* **11**, 871 (1977).
23. H. K. Allen *et al.*, *Nat. Rev. Microbiol.* **8**, 251 (2010).
24. F. Rezzonico, G. Défago, Y. Moënne-Loccoz, *Appl. Environ. Microbiol.* **70**, 5119 (2004).
25. M. W. Silby, C. Winstanley, S. A. Godfrey, S. B. Levy, R. W. Jackson, *FEMS Microbiol. Rev.* **35**, 652 (2011).
26. S. Romano *et al.*, *BMC Microbiol.* **9**, 267 (2009).
27. P. S. G. Chain *et al.*, *J. Bacteriol.* **193**, 4274 (2011).
28. C. S. Smillie *et al.*, *Nature* **480**, 241 (2011).
29. C. Walsh, *Nature* **406**, 775 (2000).

Acknowledgments: We thank R. Mitra for initial discussions regarding simulations of metagenomic assembly; T. Druley for discussions surrounding the use of the six β-lactamase control fragments; J. Fay for discussions on dating horizontal gene transfer; J. Gordon for support, thoughtful discussion, and as the advisor to A.R.; A. Moore for naming PARFuMS; and the Genome Technology Access Center at Washington University in St. Louis for generating Illumina sequence data. This work was supported by awards to G.D. through the Children's Discovery Institute (award MD-II-2011-117), the International Center for Advanced Renewable Energy and Sustainability at Washington University, and the National Academies Keck Futures Initiatives, Synthetic Biology–SB2. M.O.A.S. received funding from the Lundbeck foundation and the European Union FP7-HEALTH-2011-single-stage grant agreement 282004, EvoTAR. K.J.F. is a NSF graduate research fellow (award DGE-1143954). A.R. is the recipient of an International Fulbright Science and Technology Award. The data reported in this paper are described in the supplementary materials. Raw sequencing reads have been deposited to MG-RAST with accession nos. 4489630-39, 4489641-43, 4489645-46, 4489648-49, 4489650-51, 4489653-57, 4489659, 4489661-63, 4489665, and 4489667-68. Assembled sequences have been deposited to GenBank with accession nos. JX009202 to JX009380. The authors declare no competing financial interests.

Supplementary Materials

www.sciencemag.org/cgi/content/full/337/6098/1107/DC1
Materials and Methods
Figs. S1 to S7
Tables S1 to S19
References (*30*–*39*)

20 February 2012; accepted 22 June 2012
10.1126/science.1220761

TLR13 Recognizes Bacterial 23*S* rRNA Devoid of Erythromycin Resistance–Forming Modification

Marina Oldenburg,[1]* Anne Krüger,[1]* Ruth Ferstl,[2]*† Andreas Kaufmann,[3] Gernot Nees,[3] Anna Sigmund,[1] Barbara Bathke,[4] Henning Lauterbach,[4] Mark Suter,[4,5] Stefan Dreher,[2] Uwe Koedel,[6] Shizuo Akira,[7] Taro Kawai,[7] Jan Buer,[1] Hermann Wagner,[2] Stefan Bauer,[3] Hubertus Hochrein,[4]* Carsten J. Kirschning[1]*‡

Host protection from infection relies on the recognition of pathogens by innate pattern-recognition receptors such as Toll-like receptors (TLRs). Here, we show that the orphan receptor TLR13 in mice recognizes a conserved 23*S* ribosomal RNA (rRNA) sequence that is the binding site of macrolide, lincosamide, and streptogramin group (MLS) antibiotics (including erythromycin) in bacteria. Notably, 23*S* rRNA from clinical isolates of erythromycin-resistant *Staphylococcus aureus* and synthetic oligoribonucleotides carrying methylated adenosine or a guanosine mimicking a MLS resistance–causing modification failed to stimulate TLR13. Thus, our results reveal both a natural TLR13 ligand and specific mechanisms of antibiotic resistance as potent bacterial immune evasion strategy, avoiding recognition via TLR13.

Toll-like receptor 2 (TLR2), TLR4, and TLR9 are major host sensors of Gram-negative bacteria, and TLR2 is thought to be the central detector of Gram-positive bacteria, whereas other pattern-recognition receptors (PRRs) such as TLR7 contribute to bacteria sensing as well (*1*–*7*). However, the high sensitivity of mice lacking expression of these TLRs to Gram-positive

bacteria implies that other TLRs or members of other classes of PRRs—such as C-type lectins, RIG-I–like helicases (RLHs), or nucleotide binding domain– and leucine-rich repeat–containing receptors [NOD-like receptors (NLRs)]—play a role in the detection of Gram-positive bacteria. We therefore compared the responsiveness of macrophages lacking the expression of molecules that signal downstream of these PRRs, including caspase recruitment domain (CARD) 9, receptor-interacting protein 2, apoptosis-associated speck-like protein containing a CARD, interleukin-1 (IL-1) receptor, IL-18, or MyD88, to heat inactivated *Staphylococcus aureus* (hiSa) or *Streptococcus pneumoniae* (both Gram-positive) in the presence of a TLR2-blocking antibody (see supplementary materials and methods section) (*2*, *8*–*10*). We found that cytokine production strictly depends on MyD88 (fig. S1A), which suggests that TLRs rather than RLHs or NLRs are responsible for the detection of these bacteria. Moreover, analysis of ectopically expressed RLH function indicated a lack of RLH involvement in Gram-positive bacteria sensing (fig. S1B).

Next, we asked whether endosomal TLRs (TLR3, -7, -8, -9, -11, and -13) are involved in cell activation. We inhibited endosomal acidification with bafilomycin and analyzed UNC93B1-mutant (*3D*) macrophages that lack endoplasmic reticulum–endosome TLR trafficking and are susceptible to *S. aureus* infection (*2*, *11*, *12*). Bafilomycin treatment abrogated recognition of Gram-positive bacteria in *Tlr2*$^{-/-}$ macrophages (Fig. 1A). Furthermore, *3D/Tlr2/4*$^{-/-}$ and *3D/Tlr2*$^{-/-}$ mice or corresponding macrophages (but not those generated from *3D* mice unless TLR2 was blocked) were unresponsive to a Gram-positive bacterial challenge (Fig. 1, B and C, and fig. S1C). Unexpectedly, *Tlr23479*$^{-/-}$ macrophages (or mice) responded well to a hiSa challenge, unless the bacterial preparations were subjected to ribonuclease A (RNase A) treatment, which did not impair TLR2-driven activation of wild-type (WT) controls, or endosomal TLR function was abrogated (Fig. 1, D to F). These data suggested that an endosomal RNA sensor besides TLR3 and TLR7 can act as cellular detector of hiSa.

Dendritic cell (DC) subsets express different sets of TLRs (*13*). We generated bone marrow–derived conventional (c) DCs and plasmacytoid (p) DCs in vitro. The responsiveness of these cells to hiSa was dependent on MyD88 and UNC93B1. Specifically, *Tlr23479*$^{-/-}$ CD8^{high} (expressing TLR11, TLR12, and TLR13) and signal regulatory protein α (Sirp)^{high} cDCs (expressing TLR13 but lacking TLR11 and TLR12) responded to hiSa, whereas *Tlr23479*$^{-/-}$ pDCs (expressing TLR12 but lacking TLR11 and TLR13) failed to do so (Fig. 1G). Together, these findings imply that TLR13 acts as a bacterial single-stranded (ss) RNA sensor, even though TLR13 has recently been linked with the recognition of vesicular stomatitis virus (*14*).

To identify the relevant RNA, we incubated hiSa with calf intestinal phosphatase, 5′-phosphate–specific phosphatase [to affect the integrity of 16*S* and 23*S* ribosomal RNA (rRNA)], or double-stranded RNA–specific RNase III or VI. These treatments did not alter the stimulatory activity of hiSa, in line with a recent report (fig. S2, A to C) (*15*). However, ssRNA-specific RNase A treatment abrogated the *Tlr23479*$^{-/-}$ cDC (and macrophage) stimulatory activity of hiSa, as did nucleic acid–degrading benzonase [Fig. 1, D, E, and G, and fig. S2B; note that Flt3L-expanded CD8^{+} cDCs do not produce IL-12p70 in response to TLR2 ligands that are contained in hiSa (*16*)]. We then treated total RNA with 5′-phosphate–dependent exonuclease (to degrade specifically large rRNAs, namely 16*S* and 23*S* rRNA) and purified large rRNAs (fig. S2C) to narrow down the

[1]Institute of Medical Microbiology, University of Duisburg-Essen, 45147 Essen, Germany. [2]Institute of Medical Microbiology, Immunology and Hygiene, Technical University of Munich, 81675 Munich, Germany. [3]Institute for Immunology, Philipps University of Marburg, 35043 Marburg, Germany. [4]Department of Research Immunology, Bavarian Nordic GmbH, 82152 Martinsried, Germany. [5]Institute of Virology, University of Zurich, 8006 Zurich, Switzerland. [6]Department of Neurology, Clinic of the University of Munich, 81377 Munich, Germany. [7]World Premier International Immunology Frontier Research Center, Osaka University, Osaka 565-0871, Japan.

*These authors contributed equally to this work.
†Present address: Swiss Institute of Allergy and Asthma Research, University of Zurich, 7270 Davos, Switzerland.
‡To whom correspondence should be addressed. E-mail: carsten.kirschning@uk-essen.de

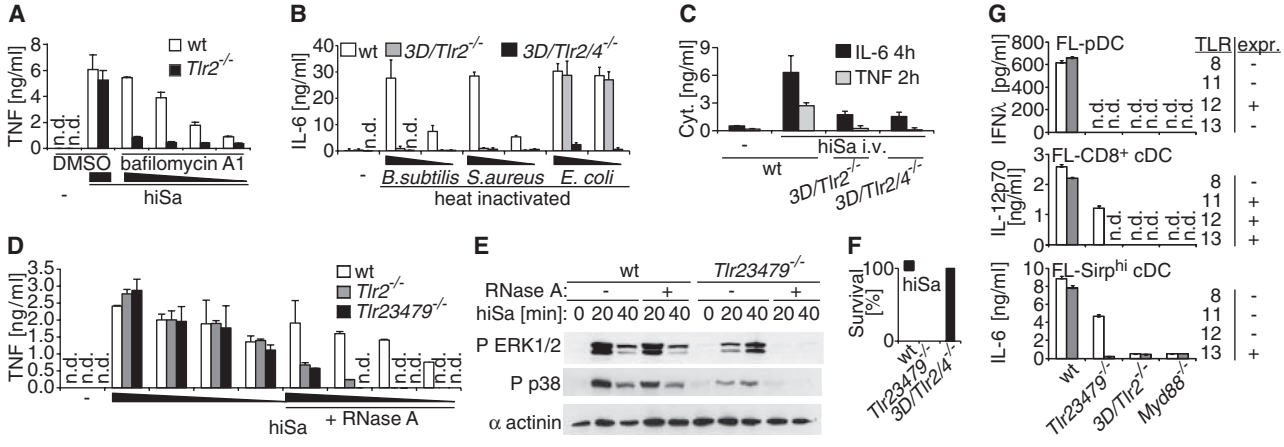

Fig. 1. Gram-positive bacteria and their RNA activate *Tlr23479*$^{-/-}$ macrophages and DCs via an unknown TLR. (**A**) Macrophages were preincubated for 30 min with dimethyl sulfoxide (DMSO) alone or 50 nM bafilomycin A1 and were challenged for 8 hours with 10^9 colony-forming units (CFU)/ml heat-inactivated *S. aureus* (hiSa; DMSO) or 10^9, 10^8, 10^7, and 10^6 CFU/ml hiSa (bafilomycin A1; -, unchallenged). Supernatants were analyzed by enzyme-linked immunosorbent assay (ELISA). n.d., not detected. (**B**) Macrophages were challenged for 16 hours with 10^9 or 10^8 CFU/ml of bacterial suspensions, whereas (**C**) corresponding mice were challenged intravenously (i.v.) with 10^9 CFU hiSa or PBS only (-) at 2 and 4 hours, upon which serum was drawn. Supernatants and serum samples were analyzed by ELISA. Cyt., cytokine; TNF, tumor necrosis factor. One out of three experiments with similar results and, respectively, $n = 3$ mice per group is illustrated as mean ± SD (error bars). (**D** and **E**) Macrophages were challenged for 16 hours (D) or for the times indicated (E) with untreated (-) or RNase A–treated (+) hiSa suspensions. (D) 10^9, 10^8, 10^7, and 10^6 or (E) 10^8 CFU/ml hiSa was used for the challenge, upon which supernatants were analyzed by ELISA or lysates were analyzed by SDS–polyacrylamide gel electrophoresis and immunoblotting. P, phosphorylated; ERK, extracellular signal–regulated kinase. (**F**) Mice were challenged by injection with hiSa (1.6×10^{11} CFU/kg body weight) and α-D-galactosamine (800 mg/kg body weight) intraperitoneally 45 min after intravenous injection of IFN-γ (50 μg/kg body weight). Survival was monitored, and all deaths occurred within 16 hours of treatment ($n = 6$ deaths per WT and *3D/Tlr2/4*$^{-/-}$ groups, $n = 4$ for *Tlr23479*$^{-/-}$ mice). (**G**) Flt3-ligand–derived DC subsets were challenged with untreated (white bars) or RNase A–treated (gray bars) hiSa at 5×10^6 CFU/ml for 16 hours. Supernatants were analyzed for cytokine contents by bead array. The respective TLR expression (expr.) in DC subsets is indicated (-, no detectable expression; +, expression). (A to E and G) For each panel, representative results from at least three experiments are shown, and each illustrated data point (A to D and G) represents mean ± SD (error bars) of duplicates.

stimulatory activity. After transfection, large rRNA isolates of both *S. aureus* and *Escherichia coli* triggered the activation of *Tlr23479*$^{-/-}$ macrophages and cDCs, whereas 16*S*/23*S* rRNA digestion abrogated stimulatory activity (Fig. 2A). Accordingly, low–molecular weight portions from total RNA lacked stimulatory activity, whereas high–molecular weight portions of Gram-positive and Gram-negative bacterial RNA activated *Tlr23479*$^{-/-}$ cells (Fig. 2B and fig. S2, D and E). These findings suggested that a fraction of large bacterial rRNAs activates macrophages and cDCs in a MyD88-dependent manner. We assume that the increased RNA-driven activation of *Tlr23479*$^{-/-}$ macrophages in comparison to WT cells reflects a lack of TLRs competing for downstream signal transduction molecules.

To analyze whether rRNA modifications induced in antibiotic-resistant strains by antibiotic treatment [e.g., with erythromycin (*17*, *18*)] would modify the immunostimulatory capacity of rRNA, we applied five clinical *S. aureus* isolates displaying various resistance phenotypes, including erythromycin resistance. Isolates grown in the presence of erythromycin largely lacked the capacity to activate *Tlr23479*$^{-/-}$ macrophages and induced lower amounts of serum cytokines early after infection (2 hours) of *Tlr23479*$^{-/-}$ mice (Fig. 2, C and D). In contrast, WT as well as *Tlr23479*$^{-/-}$ mice and corresponding macrophages responded largely normally toward the same isolate grown in the absence of erythromycin (Fig. 2, C and D, and fig. S2, F to H). The later (16 hours) increase and equalization of serum cytokine levels independent of erythromycin treatment (fig. S2H) suggested the loss of 23*S* rRNA methylation in the absence of erythromycin within the host. Together, these results demonstrate an erythromycin-driven camouflage of RNA from its receptor. Specifically, N6 methylation of rRNA adenosine (A) 2085 in *S. aureus* (corresponding to *E. coli* A2058) by the erythromycin resistance methyltransferase B (ermB) or ermC confers macrolide, lincosamide, and streptogramin group (MLS) antibiotic (including erythromycin) resistance (*17*, *18*). Accordingly and also in line with the inducibility of erm expression by erythromycin (*17*, *18*), 23*S* rRNA from *S. aureus* grown in erythromycin failed to stimulate *Tlr23479*$^{-/-}$ macrophages (Fig. 2E). In contrast, 23*S* rRNA from resistant *S. aureus* not grown in erythromycin and 23*S* rRNA from *E. coli* (including enterohemorrhagic *E. coli*) activated *Tlr23479*$^{-/-}$ macrophages, whereas the respective 16*S* rRNAs failed to do so (Fig. 2E and fig. S2, I and J). Moreover, overexpression of ermB and ermC (the latter being subcloned from cDNA of an erythromycin-grown *S. aureus* isolate) in *E. coli* and *Bacillus subtilis* strains not only conferred erythromycin resistance but also ablated 23*S* rRNA stimulatory activity (Fig. 2F and fig. S2K). These data indicate that resistance to MLS group antibiotics (including erythromycin) mediated by site-specific methylation (targeting A2085 in *S. aureus* and A2058 in *E. coli* 23*S* rRNA) rendered 23*S* rRNA nonstimulatory.

To address the immune stimulatory activity of 23*S* rRNA in more detail, we designed three oligoribonucleotides (ORNs) as analogs of *S. aureus* 23*S* rRNA segments, each of which carries an A in its center that becomes methylated constitutively or under growth restriction to modulate the docking of protein synthesis cofactors or antibiotics. The three ORNs named SaI, SaII, and SaIII represented *S. aureus* A1662 [*E. coli* A1616, methylation of which promotes fitness (*19*)], *S. aureus* A2530 [*E. coli* A2503, targeted by chloramphenicol, florfenicol, and clindamycin resistance RNA methyltransferase (*20*)], and *S. aureus* A2085 [*E. coli* A2058, modification of which costs fitness (*17*, *18*, *21*)], respectively (table S1).

Only SaIII (which mirrors *S. aureus* A2085) activated *Tlr23479*$^{-/-}$ cells (Fig. 3A). pDCs recognized SaIII via TLR7, but this activity was lost with 3′-terminal deletion (fig. S3). ORNs resulting from deletions of 3′- and 5′-termini (SaIIId3, SaIIId5, Sa23) equally activated *Tlr23479*$^{-/-}$ cDCs (Fig. 3B), whereas preincubation of *S. aureus* RNA or of ORN Sa23 with an antisense SaIII RNA strand (SaIIIas) abrogated the stimulatory activity (Fig. 3C). These results indicated single-strand structure and singularity of the stimulatory activity within the bacterial transcriptome. Successive terminal deletions toward a 12-mer ORN (Sa12, table S1) led to sequences that were identical in *S. aureus* and *E. coli* 23*S* rRNAs. Length-dependent reduction of stimulatory capacity could largely be compensated by terminal fill-ups (Sa12A19, Fig. 3D) (*22*). Upon N6 methylation at A6 (corresponding to *S. aureus* A2085 and mimicking erm-methylated 23*S* rRNA), Sa12 lacked stimulatory capacity, whereas N6 methylation at A7 merely caused a partial reduction (Fig. 3E). Consecutive single substitutions of Sa12 revealed "CGGAAAGACC" as the minimal stimulatory segment because ORNs with substitutions at position one or two of Sa12 (Sa12s1 and Sa12s2) were fully stimulatory, whereas further substitutions resulted in drastic loss (Sa12s10 and Sa12s12) or abrogation of the stimulatory activity (Fig. 3F and table S1).

In contrast, Sa12 derivatives mimicking eukaryotic 28*S* rRNA or specific 23*S* rRNA mutations that render bacteria resistant to MLS antibiotics

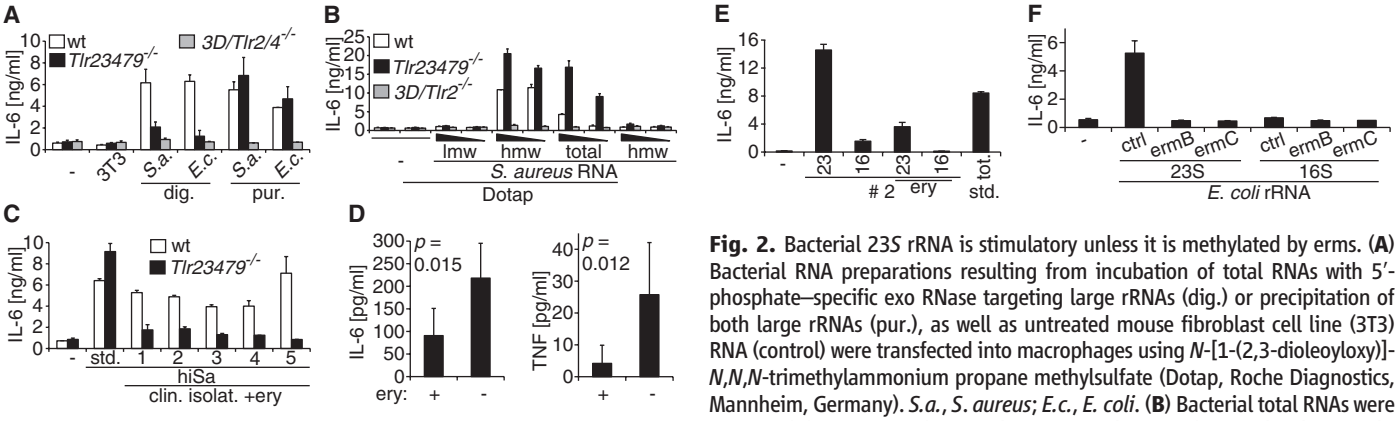

Fig. 2. Bacterial 23*S* rRNA is stimulatory unless it is methylated by erms. (**A**) Bacterial RNA preparations resulting from incubation of total RNAs with 5′-phosphate–specific exo RNase targeting large rRNAs (dig.) or precipitation of both large rRNAs (pur.), as well as untreated mouse fibroblast cell line (3T3) RNA (control) were transfected into macrophages using *N*-[1-(2,3-dioleoyloxy)]-*N*,*N*,*N*-trimethylammonium propane methylsulfate (Dotap, Roche Diagnostics, Mannheim, Germany). *S.a.*, *S. aureus*; *E.c.*, *E. coli*. (**B**) Bacterial total RNAs were separated by anion-exchange chromatography into low–molecular weight (lmw) and high–molecular weight (hmw) fractions, which were used to challenge macrophages with or without Dotap transfection. (**C**) Macrophages were challenged with 10^9 CFU/ml erythromycin-sensitive (std.) hiSa or five erythromycin-resistant clinical *S. aureus* isolates cultured in 10 mg/liter erythromycin (clin. isolat. +ery). (A to C) Supernatants were analyzed 16 hours poststimulation using ELISA. (**D**) *Tlr23479*$^{-/-}$ mice were infected i.v. with 10^8 CFU erythromycin-resistant *S. aureus* clinical isolate growing logarithmically in the presence (+) or absence (-) of erythromycin. Serum was drawn after 2 hours and analyzed for cytokines by cytometric bead array. Mean ± SD (error bars) for $n = 6$ mice per each group is shown. (**E**) Total (tot.) RNA from erythromycin-sensitive *S. aureus* (std.) and agarose gel–purified 16*S* (16) and 23*S* (23) rRNAs from clinical isolate 2 grown in the absence or presence of erythromycin (ery) were transfected into *Tlr23479*$^{-/-}$ macrophages using Lyovec (Cayla-InvivoGen, Toulouse, France). (**F**) *E. coli* BL21 was transformed with empty vector control (ctrl) or ermB or ermC expression plasmids. After 16 hours, culture of 16*S* and 23*S* rRNA was isolated and transfected into *Tlr23479*$^{-/-}$ macrophages. (E and F) Supernatants were analyzed 16 hours postchallenge using ELISA. (A to C, E, and F) Each panel illustrates a representative result of three independent experiments and depicts means ± SD (error bars) of duplicate samples. For (D), one statistically significant experiment has been performed ($P \leq 0.015$).

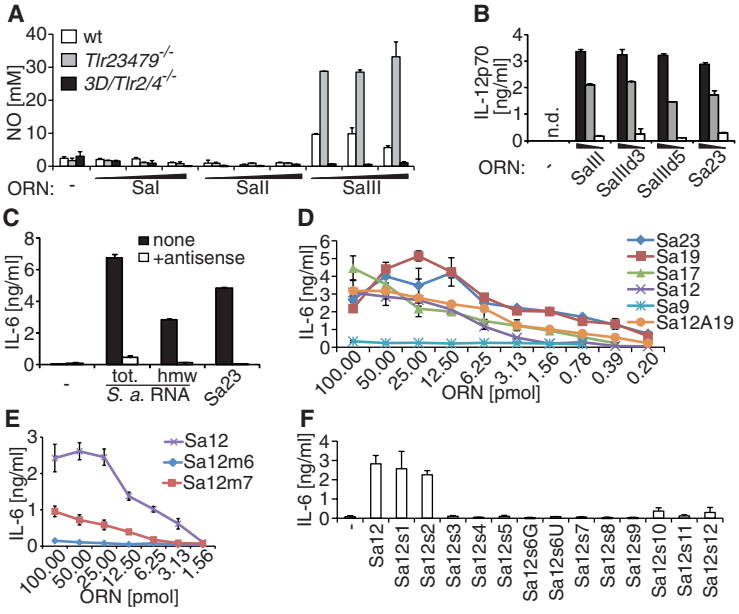

Fig. 3. Oligoribonucleotides (ORNs) covering the erm target site in 23*S* rRNA (region around A2085 in *S. aureus*/2058 in *E. coli*) activate macrophages and cDCs. (**A**) Sequence motifs covering three separate methylation sites in *S. aureus* 23*S* rRNA were mirrored by ORNs (see table S1). Macrophages were challenged with 1, 10, and 100 pmol per well of the ORNs. NO, nitrite. (**B**) *Tlr23479*$^{-/-}$ FL-CD8^{+} cDCs were transfected with the ORNs indicated (amount per well [pmol]: black, 10; gray, 1; white, 0.1). (**C**) *Tlr23479*$^{-/-}$ Sirp^{high} cDCs were transfected with 100 ng per well of the *S. aureus* RNA preparations indicated or an ORN covering the SaIII core sequence (10 pmol per well), either in the absence of (none) or upon preincubation for 20 min with 100 pmol per well antisense RNA ORN (SaIIIas, +antisense). (**D** to **F**) Undifferentiated bone marrow cells were challenged with ORNs at the doses per well indicated in (D) and (E) or 100 pmol per well (F). (A to F) Cells were transfected [(A) Dotap, (B to F) Lyovec] for 16 hours with the indicated RNAs and ORNs. In each experiment, supernatants were assayed for nitrite content by Griess assay (A) or proinflammatory cytokine contents by bead assay (B and C) or ELISA (D to F). Each panel illustrates a representative result of three independent experiments and depicts means ± SD (error bars) of duplicate samples (A to E) or the mean ± SD of at least three independent experiments (F).

(*S. aureus* 23*S* rRNA A2085G, mimicked by ORN Sa12s6G or Sa12s6U) failed to stimulate bone marrow cells (Fig. 3F and table S1) (*18*, *23*). These findings suggest that molecular mechanisms rendering bacteria resistant to naturally occurring antibiotics also impede MyD88-dependent host recognition by an ill-defined endosomal TLR.

To characterize the responsible TLR, we focused on TLR13, because analysis of *Tlr8*$^{-/-}$ macrophages ruled out the involvement of TLR8. Specifically, WT and *Tlr8*$^{-/-}$ macrophages exhibited comparable response to hiSa upon blockade of TLR7, TLR9, and TLR2. Moreover, responsiveness to 23*S* rRNA–derived SaIII was similar (fig. S4A). Notably, small interfering RNA (siRNA)–driven suppression of TLR13 mRNA accumulation impaired the recognition of stimulatory ORNs such as SaIII by *Tlr23479*$^{-/-}$ macrophages (Fig. 4A). Although recognition of low doses of hiSa by *Tlr23479*$^{-/-}$ macrophages treated with siRNA for TLR13 was strongly impaired, high-dose hiSa challenge activated not only control but also TLR13 siRNA-treated cells, presumably via unsuppressed TLR13 molecules (fig. S4B). In addition, knockdown of MAPK1 mRNA indicated involvement of MAPK1 in TLR13-driven signal transduction (Fig. 4A and fig. S4B). Furthermore, ectopic expression of TLR13 but not of CD14, TLR3, -7, -8, -9, or -12 conferred responsiveness of human embryonic kidney (HEK) 293 cells toward hiSa or the ORNs SaIII, Sa23, Sa17, or Sa12 (Fig. 4, B to D, and fig. S4, C and D). Other ORNs such as RNA40 (TLR7 ligand) or CpG-containing oligodeoxynucleotides (ODNs) (TLR9 ligands) were inactive (Fig. 4E).

Having identified the conserved 23*S* rRNA sequence "CGGAAAGACC" as a ligand for TLR13,

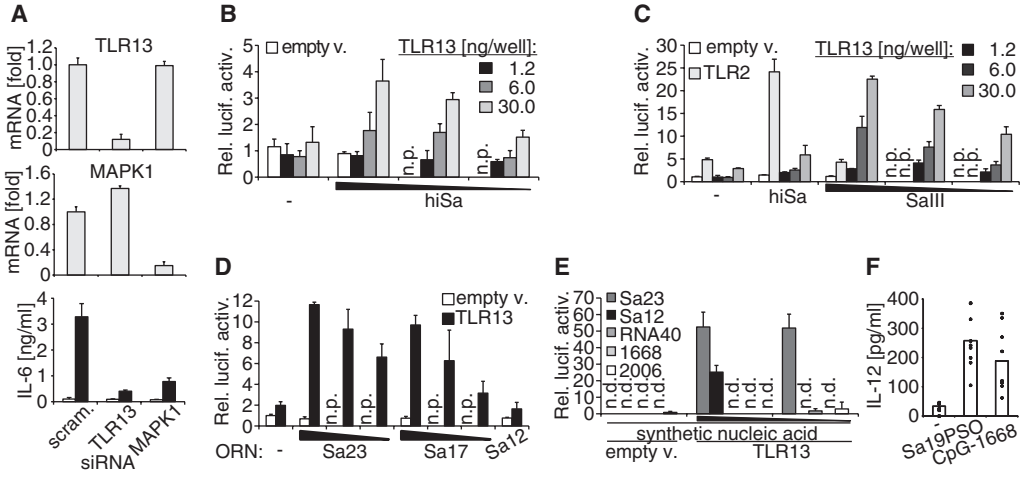

Fig. 4. TLR13 recognizes heat-inactivated *S. aureus* and ORNs mirroring bacterial 23*S* rRNA segments covering A2085/2058. (**A**) 5×10^5 *Tlr23479*$^{-/-}$ macrophages were transfected with 50 pmol mRNA-specific siRNAs or scrambled control siRNA (scram.). After 48 hours, cells were challenged for 16 hours with 100 pmol per well ORN SaIII (black columns, bottom) or left untreated (white columns, bottom), and supernatants were analyzed by ELISA (bottom). Untreated cells were lysed to isolate mRNA, and levels of corresponding mRNAs were determined by reverse transcription polymerase chain reaction (top and middle). (**B** to **E**) HEK293 line cells were transfected with control, TLR2, or TLR13 expression and luciferase reporter plasmids. In general, cells were transfected with 15 ng empty vector (empty v.), 2 ng TLR2 (C), 15 ng TLR13 (D and E), or the amounts of TLR13 expression plasmid indicated in (B) and (C). At 24 hours posttransfection, cells were challenged with 10^9, 10^8, and 10^7 CFU/ml of hiSa (B); 10^9 CFU/ml hiSa (C); 100, 10, and 1 pmol per well ORN (C and D); 100 pmol per well ORN only (D and E); or 100 and 10 pmol per well ORN (E). Either 10 μM of oligodeoxynucleotides (ODN, 1668 and 2006) only or 10 and 1 μM of ODN was applied. ORN RNA40 was transfected with the reagent Dotap (E). After incubation for 16 hours, NF-κB–driven relative luciferase activity (rel. lucif. activ.) was analyzed. n.p., not performed; -, no challenge. (A to E) Each panel illustrates a representative result of three experiments and depicts means ± SD (error bars) of triplicate samples. (**F**) WT mice were challenged by i.v. injection of 10 nmol of ORN or ODN (n = 9 mice per group) in 200 μl PBS or PBS alone (-). Serum was drawn 6 hours later and analyzed for IL-12p70 content by cytometric bead arrays (IL-12). Combined data of three experiments in which three mice per group were applied are shown as the mean of individual results.

we set out to evaluate its importance in vivo. Therefore, we compared the cytokine storm induced by systemic application of TLR13-activating ORNs with that of TLR9-activating CpG-ODNs. Application of a nuclease-resistant phosphorothioate Sa19 variant (Sa19 PSO) in vivo triggered systemic proinflammatory cytokine release similar to that elicited by the PSO-CpG oligonucleotide 1668 (Fig. 4F and fig. S4, E and F). Consequently, systemic application of Sa19PSO to mice along with interferon-γ (IFN-γ) and D-galactosamine sensitization induced a fatal, septic shock–like syndrome in mice with functional TLR13 (WT and *Tlr23479*$^{-/-}$), whereas the *3D*/*Tlr24*$^{-/-}$ mice that lack responsiveness to TLR13 were resistant (fig. S4G), concordant with the genotype-selective fatal pathology elicited by systemic challenge with hiSa (Fig. 1F). In contrast to the ORN Sa19, an ODN version of Sa19 (Sa19DNA, containing two CpG motifs) lacked TLR13 stimulatory activity but activated TLR9 (fig. S4F). Together, these data indicate that TLR13 functions as an important bacteria sensor by recognizing an ssRNA segment within the peptidyl transferase loop of bacterial 23*S* rRNA that binds antibiotics of the MLS group.

Our data unravel an unanticipated link between antibiotic resistance and evasion from TLR13 recognition, because 23*S* rRNA modifications generating resistance toward MLS antibiotics also camouflaged bacteria from TLR13 recognition. MLS antibiotic-producing bacteria such as *Saccharopolyspora erythraea* were possibly first to express erms (to resist their own antibiotics) (*17*). Erm expression plasmids might have been acquired from *S. erythraea* by staphylococci, pneumococci, and mycobacteria (which seem to accompany or even correlate with the tuberculous property of the latter) (*17*, *24*). Though macrolide resistance appears to be associated with fitness costs (*21*), the pathogenic recipients did gain invisibility to TLR13. We therefore speculate that widespread ancient antibiotic resistance (*25*) has subverted TLR13-driven antibacterial immune resistance, which may explain why TLR13 expression has been abandoned in certain mammalian species, including humans. If so, we anticipate that, in humans, the function of TLR13 has been replaced by an RNA-sensing PRR that is able to still recognize erythromycin resistance–forming RNA modifications.

References and Notes

1. A. Iwasaki, R. Medzhitov, *Science* **327**, 291 (2010).
2. T. Kawai, S. Akira, *Immunity* **34**, 637 (2011).
3. H. D. Brightbill *et al.*, *Science* **285**, 732 (1999).
4. H. Hemmi *et al.*, *Nature* **408**, 740 (2000).
5. K. Crozat, B. Beutler, *Proc. Natl. Acad. Sci. U.S.A.* **101**, 6835 (2004).
6. K. Karikó, M. Buckstein, H. Ni, D. Weissman, *Immunity* **23**, 165 (2005).
7. G. Mancuso *et al.*, *Nat. Immunol.* **10**, 587 (2009).
8. J. Ruland, *Ann. N. Y. Acad. Sci.* **1143**, 35 (2008).
9. S. E. Girardin *et al.*, *J. Biol. Chem.* **278**, 8869 (2003).
10. R. Muñoz-Planillo, L. Franchi, L. S. Miller, G. Núñez, *J. Immunol.* **183**, 3942 (2009).
11. K. Tabeta *et al.*, *Nat. Immunol.* **7**, 156 (2006).
12. M. M. Brinkmann *et al.*, *J. Cell Biol.* **177**, 265 (2007).
13. C. A. Luber *et al.*, *Immunity* **32**, 279 (2010).
14. Z. Shi *et al.*, *J. Biol. Chem.* **286**, 4517 (2011).
15. S. D. Deshmukh *et al.*, *EMBO Rep.* **12**, 71 (2011).
16. H. Lauterbach *et al.*, *J. Exp. Med.* **207**, 2703 (2010).
17. R. H. Skinner, E. Cundliffe, *J. Gen. Microbiol.* **128**, 2411 (1982).
18. B. Weisblum, *Antimicrob. Agents Chemother.* **39**, 577 (1995).
19. P. V. Sergiev, M. V. Serebryakova, A. A. Bogdanov, O. A. Dontsova, *J. Mol. Biol.* **375**, 291 (2008).
20. K. S. Long, J. Poehlsgaard, C. Kehrenberg, S. Schwarz, B. Vester, *Antimicrob. Agents Chemother.* **50**, 2500 (2006).
21. P. Pfister *et al.*, *Proc. Natl. Acad. Sci. U.S.A.* **102**, 5180 (2005).
22. V. Hornung *et al.*, *Nat. Med.* **11**, 263 (2005).
23. S. Klinge, F. Voigts-Hoffmann, M. Leibundgut, S. Arpagaus, N. Ban, *Science* **334**, 941 (2011).
24. K. Buriánková *et al.*, *Antimicrob. Agents Chemother.* **48**, 143 (2004).
25. V. M. D'Costa *et al.*, *Nature* **477**, 457 (2011).

Acknowledgments: We thank S. Schimanski, J. Pätzold, R. Kassub, T. Scholtysik, and P. Juszczak, as well as C. Chebrolu for technical work; M. Freudenberg, J. Steinmann, and J. Kehrmann for provision of mice and bacteria; R. Lang for advice; the German research foundation (Deutsche Forschungsgemeinschaft) for funding of KI 591/4-1 and GK1045 (to C.J.K.) and BA 1618/5-1 (to S.B.), as well as to U.K.; and the Japanese Government for funding to S.A. and T.K. The Behring Röntgen Stiftung funded grant 56-0034 (to S.B.). The Univ. of Duisburg-Essen (C.J.K.), Bavarian Nordic GmbH (H.H.), and the Philipps Univ. of Marburg (S.B.) filed a patent on TLR13 activators (U.S. Patent 61/597,063; agonists and antagonists of TLR13). H.W. and S.B. had an advisory contract with Coley Pharmaceuticals/Pfizer that ended in 2010. The data presented in this paper are tabulated in the main paper and in the supplementary materials.

Supplementary Materials

www.sciencemag.org/cgi/content/full/science.1220363/DC1
Materials and Methods
Supplementary Text
Figs. S1 to S4
Table S1
References (*26*–*32*)

10 February 2012; accepted 3 July 2012
Published online 19 July 2012;
10.1126/science.1220363

Compartmentalized Control of Skin Immunity by Resident Commensals

Shruti Naik,[1,2] Nicolas Bouladoux,[1] Christoph Wilhelm,[1] Michael J. Molloy,[1] Rosalba Salcedo,[3,4] Wolfgang Kastenmuller,[5] Clayton Deming,[6] Mariam Quinones,[7] Lily Koo,[8] Sean Conlan,[6] Sean Spencer,[1,2] Jason A. Hall,[9] Amiran Dzutsev,[3,4] Heidi Kong,[10] Daniel J. Campbell,[11,12] Giorgio Trinchieri,[3] Julia A. Segre,[6] Yasmine Belkaid[1]*

Intestinal commensal bacteria induce protective and regulatory responses that maintain host-microbial mutualism. However, the contribution of tissue-resident commensals to immunity and inflammation at other barrier sites has not been addressed. We found that in mice, the skin microbiota have an autonomous role in controlling the local inflammatory milieu and tuning resident T lymphocyte function. Protective immunity to a cutaneous pathogen was found to be critically dependent on the skin microbiota but not the gut microbiota. Furthermore, skin commensals tuned the function of local T cells in a manner dependent on signaling downstream of the interleukin-1 receptor. These findings underscore the importance of the microbiota as a distinctive feature of tissue compartmentalization, and provide insight into mechanisms of immune system regulation by resident commensal niches in health and disease.

Mammals and their microbiota have formed an evolutionary partnership that is critical for metabolism, tissue development, and host defense (*1*–*3*). In particular, the gut flora has been implicated in intestinal immune tissue development and function, as well as in promoting systemic inflammation in the context of autoimmunity and infection (*1*, *4*–*8*). Despite our growing understanding of the consequences of this host-microbe alliance for intestinal immune function, the degree to which the gut flora contributes to immunity at distal sites remains unclear.

The skin represents the primary interface between the host and the environment. Microbial

[1]Mucosal Immunology Section, Laboratory of Parasitic Diseases, National Institute of Allergy and Infectious Diseases, Bethesda, MD 20892, USA. [2]Immunology Graduate Group, University of Pennsylvania, Philadelphia, PA 19104, USA. [3]Cancer and Inflammation Program, Center for Cancer Research, National Cancer Institute, Frederick, MD 21702, USA. [4]SAIC-Frederick Inc., National Cancer Institute, Frederick, MD 21701, USA. [5]Lymphocyte Biology Section, Laboratory of Immunology, National Institute of Allergy and Infectious Diseases, Bethesda, MD 20892, USA. [6]Genetics and Molecular Biology Branch, National Human Genome Research Institute, Bethesda, MD 20892, USA. [7]Bioinformatics and Computational Biosciences Branch, National Institute of Allergy and Infectious Diseases, Bethesda, MD 20892, USA. [8]Research Technology Branch, National Institute of Allergy and Infectious Diseases, Bethesda, MD 20892, USA. [9]Molecular Pathogenesis Program, Kimmel Center for Biology and Medicine, Skirball Institute of Biomolecular Medicine, New York University School of Medicine, New York, NY 10016, USA. [10]Dermatology Branch, Center for Cancer Research, National Cancer Institute, Bethesda, MD 20892, USA. [11]Benaroya Research Institute, Seattle, WA 98101, USA. [12]Department of Immunology, University of Washington School of Medicine, Seattle, WA 98195, USA.

*To whom correspondence should be addressed. E-mail: ybelkaid@niaid.nih.gov